

RESEARCH ARTICLE

Proteomic analysis reveals higher demand for antioxidant protection in embryonic stem cell-derived smooth muscle cells

Xiaoke Yin¹, Manuel Mayr¹, Qingzhong Xiao¹, Wen Wang² and Qingbo Xu¹

¹ Cardiovascular Division, School of Medicine, King's College, University of London, UK

² Medical Engineering Division, Department of Engineering, Queen Mary, University of London, London, UK

Embryonic stem (ES) cells can differentiate into vascular smooth muscle cells (SMCs), but differences in protein composition, function and behaviour between stem cell-derived and mature SMCs remain to be characterized. Using differential in gel electrophoresis (DIGE) and MS, we identified 146 proteins that differed between ES cell-derived SMCs (esSMCs) and aortic SMCs, including proteins involved in DNA maintenance (higher in esSMCs), cytoskeletal proteins and calcium-binding proteins (higher in aortic SMCs). Notably, esSMCs showed decreased expression of mitochondrial, but a compensatory increase of cytosolic antioxidants. Subsequent experiments revealed that mitochondrial-derived reactive oxygen species (ROS) were markedly increased in esSMCs. Despite a three-fold rise in glutathione (GSH) reductase activity, esSMCs had lower levels of reduced GSH, and depletion of GSH by diethyl maleate or inhibition of GSH reductase by carmustine (BCNU) resulted in more pronounced cell death compared to aortic SMCs, while addition of antioxidants improved the viability of esSMCs. We present the first proteomic analysis of esSMCs demonstrating that stem cell-derived SMCs are more sensitive to oxidative stress due to increased generation of mitochondrial-derived ROS and require additional antioxidant protection for survival.

Received: May 10, 2006
Revised: August 17, 2006
Accepted: August 21, 2006

**Keywords:**

Antioxidant / Differentiation / Embryonic stem cell / Mitochondria / Smooth muscle cell

1 Introduction

Embryonic stem (ES) cells are the pluripotent derivatives of the inner cell mass of blastocysts [1, 2]. They have the capacity for unlimited growth and self-renewal and the ability to

differentiate into all types of cells including germ cells. Over the last few years, accumulating evidence indicates that stem cells can differentiate into smooth muscle cells (SMCs) [3–7]. Advances in cell biology, microtechnology and biomaterial sciences have generated new opportunities to create tissues from stem cells replacing injured or diseased organs. A number of studies have been performed to engineer vascular tissues by seeding vascular cells including SMCs and endothelial cells onto 3-D, biodegradable synthetic [8–11] or natural [12, 13] polymer scaffolds, and by allowing the cell-scaffold constructs to develop into new vascular tissues *in vitro* or *in vivo*. For this purpose, stem cell-derived SMCs could be an important source for tissue engineering and for vessel repair.

Recent developments of proteomic techniques provide powerful tools for studying protein alterations and molecular mechanisms of cell function [14]. To date, three protein maps of vascular SMCs have been published: McGregor *et al.* [15]

Correspondence: Dr. Manuel Mayr, Cardiovascular Division, School of Medicine, King's College, University of London, 125 Coldharbour Lane, London SE5 9NU, UK

E-mail: manuel.mayr@kcl.ac.uk

Fax: +44-20-3299-3510

Abbreviations: DEM, diethyl maleate; DM, differentiation medium; ES, embryonic stem; esSMC, ES cell-derived smooth muscle cell; FACS, fluorescent-activated cell sorting; GSH, glutathione; PDGF, platelet-derived growth factor; PRX, peroxiredoxin; ROS, reactive oxygen species; Sca-1, stem cell antigen-1; SMC, smooth muscle cell; SOD, superoxide dismutase

characterized venous SMCs by dissecting the media from human saphenous veins, while Dupont *et al.* [16] analysed the proteome and secretome of cultured arterial SMCs obtained from human internal mammary arteries. Similarly, we have previously mapped the proteome of mouse aortic SMCs [17] and their stem cell antigen-1 positive (Sca-1⁺) progenitor cells [18], which can be derived from ES cells or adult adventitial tissues [7] and differentiated to SMC-like cells. However, no data exist on whether stem cell-derived SMCs differ functionally from mature SMCs from adult vessels, and it is unclear as to how much similarity both cell types share at the protein level. In the present study, we differentiated murine ES cells into SMCs and compared their protein expression to aortic SMCs using the DIGE approach [19], which allows accurate quantification of protein changes during cell differentiation.

2 Materials and methods

2.1 Differentiation of ES cells

Murine ES cells (ES-D3 cell line, CRL-1934 and ATCC) were maintained as described previously [20] in DMEM (ATCC) containing 10% fetal bovine serum (FBS, ATCC), 10 ng/mL recombinant human leukaemia inhibitory factor (LIF, Chemicon), 0.1 mM 2-mercaptoethanol (Sigma), 2 mM L-glutamine (Invitrogen, San Diego, CA, USA), 100 U/mL of penicillin (Invitrogen) and 100 µg/mL of streptomycin (Invitrogen). Undifferentiated ES cells were incubated at 37°C in a humidified atmosphere with 5% CO₂, and passaged into flasks coated with 0.04% gelatine (Sigma) at a ratio of 1:6 to 1:10 every 2 days. During the differentiation process, ES cells were first predifferentiated in collagen type IV (Trevigen)-coated flasks for 3–4 days in basic differentiation medium (DM): α -minimal essential medium (α MEM, Invitrogen), supplemented with 10% FCS (Invitrogen), 50 µM 2-mercaptoethanol (Sigma), 2 mM L-glutamine (Invitrogen), 100 U/mL of penicillin (Invitrogen) and 100 µg/mL of streptomycin (Invitrogen). Sca-1⁺ cells were isolated by magnetic labelling cell sorting (MACS) using anti-Sca-1 magnetic beads (Miltenyi Biotec) as described in our previous studies [7]. Sca-1⁺ cells were resuspended in fresh DM with 10 ng/mL platelet-derived growth factor (PDGF)-BB (Sigma). After five passages, a panel of SMC markers was detected in ES cell-derived SMCs (esSMCs) by fluorescent-activated cell sorting (FACS), immunofluorescent staining and reverse transcription PCR. After PDGF withdrawal, esSMCs were continuously cultivated for at least another ten passages in basic DM before they were used for experiments.

2.2 SMC culture

Mouse vascular SMCs of C57BL/6J mice (Charles River, Sulzfeld, Germany) were isolated from aortas by enzymatic digestion as described previously [21]. They were cultured in

the same condition as esSMCs and harvested for experiments on passages 15–30.

2.3 Reverse transcription-PCR

Total RNA was extracted from cells using RNeasy kit (Qiagen, Valencia, CA, USA) according to the manufacturer's instructions. Reverse transcription was performed using an Improm-IITM RT kit (Promega, Madison, WI, USA). cDNA (50 ng) was used in a PCR kit (Invitrogen) following the manufacturer's instructions. Oligonucleotide primer sequences were as follows: smooth muscle alpha-actin (SMA): forward: 5'-ACGGCCGCTCCTCTTCCTC-3', reverse: 5'-GCCCAGCTTCGTCGTATTCC-3'; smooth muscle protein 22 (SM22): forward: 5'-GCAGTCCAAAATTGAAGA-3', reverse: 5'-CTGTTGCTGCCATTTGAAG-3'; smooth muscle myosin heavy chain (SMMHC): forward: 5'-ATCTTCTACTACCTGCTCGC-3', reverse: 5'-CGGCTGAATCCATCGGAA-3'; h1-calponin (CAL): forward: 5'-TAA-CCGAGGTCCTGCCTACG-3', reverse: 5'-TGTGGGTGGGCTCACTCAGC-3'; glyceraldehyde-3-phosphate dehydrogenase (GAPDH): forward: 5'-CGGAGTCAACGGATTTGGTCGTAT-3', reverse: 5'-AGCCTTCTCCATGGTGGTGAA-GAC-3'.

2.4 Flow cytometry analysis

The procedure used for flow cytometry was similar to that described previously [7]. Briefly, cells were incubated in diluted serum (the species of serum is the same as the secondary antibody which was used) for 20 min on ice to block any nonspecific antibody binding. The single-cell suspension was aliquoted and incubated with either isotype control or SMA (C6198, Sigma), calponin (C2687, Sigma) and SMMHC (M7786, Sigma) antibodies for 30 min on ice, followed by incubation with rabbit antimouse Ig conjugated with FITC (DAKO) or rabbit antirat Ig conjugated with FITC (DAKO). Cell suspensions were analysed with a FACS scan flow cytometer (Becton Dickinson Immunocytometry Systems, Mountain View, CA, USA). Forward and 90° side scatter were used to identify and gate the positive and negative populations. Data analysis was carried out using CellQuest software (Becton Dickinson).

2.5 DIGE

Protein extracts were prepared from aortic SMCs and esSMCs using a lysis buffer (8 M urea, 4% w/v CHAPS, 30 mM Tris-Cl, pH 8.5) compatible with DIGE labelling (GE healthcare). After centrifugation at 13 000 × g for 10 min, the supernatant containing soluble proteins was harvested and the protein concentration was determined using a modification of the method described by Bradford [22]. The fluorescence dye labelling reaction was carried out at a dye/protein ratio of 400 pmol *per* 100 µg. After incubation on ice for 30 min, the labelling reaction was

stopped by scavenging nonbound dyes with 10 mM lysine (L8662, Sigma) for 15 min. For 2-DE, samples were mixed with 2× buffer (8 M urea, 4% w/v CHAPS, 2% w/v DTT, 2% v/v Pharmalytes, pH 3–10, for IEF), 50 µg *per* sample was diluted in rehydration solution (8 M urea, 0.5% w/v CHAPS, 0.2% w/v DTT and 0.2% v/v Pharmalyte, pH 3–10) and loaded on IPG strips (18 cm, pH 3–10, nonlinear, GE healthcare). After rehydration overnight, strips were focused at 0.05 mA/IPG strip for 60 kV·h at 20°C (Multiphor II, GE healthcare). Once IEF was complete, the strips were equilibrated in 6 M urea containing 30% v/v glycerol, 2% w/v SDS and 0.01% w/v Bromphenol blue, with the addition of 1% w/v DTT for 15 min, followed by the same buffer without DTT, but with the addition of 4.8% w/v iodoacetamide for 15 min. SDS-PAGE was performed using 12% T (total acrylamide concentration), 2.6% C (degree of crosslinking) polyacrylamide gels without a stacking gel, using the Ettan DALT system (GE healthcare). The second dimension was terminated when the Bromophenol blue dye front had migrated off the lower end to the gels. After electrophoresis, fluorescence images were acquired using the Typhoon variable mode imager 9400 (GE healthcare). Finally, gels were fixed overnight in methanol/acetic acid/water solution (4:1:5 v/v/v). Protein profiles were visualized by silver staining using the Plus one silver staining kit (GE healthcare) with slight modifications [23] to ensure compatibility with subsequent MS analysis. For documentation, silver-stained gels were scanned in transmission scan mode using a calibrated scanner (GS-800, BioRad). Detailed protocols can be downloaded from our website (<http://www.vascular-proteomics.com>).

2.6 MS

Differences in protein expression were analysed using the DeCyder[®] software (GE healthcare). Spots showing a statistically significant difference in intensity were excised and treated overnight with Sequencing Grade Modified Trypsin (V5111, Promega) according to a published protocol [24]. Peptide fragments were recovered by sequential extractions with 100 mM ammonium bicarbonate and extraction solution (5% v/v formic acid, 50% ACN). Extracts were lyophilized, resuspended in 10 µL of 0.1% v/v TFA and desalted with µC-18 ZipTip (Millipore) according to the manufacturer's instructions. MALDI-TOF MS was performed using an Axima CFR spectrometer (Kratos, Manchester, UK). The instrument was operated in the positive ion reflectron mode. Sample (1 µL) and 1 µL of matrix (10 mg CHCA in 300 µL of 0.1% TFA and 700 µL of ACN) were applied. The spectra were analysed using the Kompact software (version 2.3.4, Kratos) and the prominent peaks were labelled and internally calibrated using trypsin autolysis products (monoisotopic masses at $m/z = 842.51$, 1045.56 and 2211.10). Their peptide masses were searched against Swiss-Prot databases using the MASCOT program [25]. One missed cleavage

per peptide was allowed and carbamidomethylation of cysteine as well as partial oxidation of methionine were assumed.

For MS/MS, in-gel digestion with trypsin was performed according to published methods [24, 26] modified for use with an Investigator ProGest (Genomic Solutions) robotic digestion system. Following enzymatic degradation, peptides were separated by capillary LC on an RP column (BioBasic-18, 100 mm × 0.18 mm, particle size 5 µm, Thermo Electron Corporation) and applied to an LCQ ion-trap mass spectrometer (LCQ Deca XP Plus, Thermo Electron Corporation). Spectra were collected from the ion-trap mass analyser using full ion scan mode over the m/z range 300–1800. MS–MS scans were performed on each ion using dynamic exclusion. Database searches were performed using the TurboSE-QUEST software (Bioworks Browser version 3.2, Thermo Electron Corporation) against UniProt database. Following filter was applied: for charge state 1, $X_{\text{Corr}} > 1.50$; for charge state 2, $X_{\text{Corr}} > 2.00$; and for charge state 3, $X_{\text{Corr}} > 2.50$.

2.7 Immunoblotting

Cellular protein extracts were harvested according to an established protocol. Immunoblotting was performed as described previously [27, 28]. The following antibodies were used: actin (sc-1616, 1:1000, Santa Cruz), myosin light chain-1 (ab680, 1:1000, Abcam), α -tubulin (ab7750, 1:100, Abcam), heat shock protein 90 (sc-7947, 1:300, Santa Cruz), heat shock protein 70 (SPA-810, Stressgen), heat shock protein 60 (SPA-807, 1:400, Stressgen), heat shock protein 47 (ab13510, 1:1000, Abcam), heat shock protein 27 (sc-1049, 1:1000, Santa Cruz), crystallin α/β (ab13497, 1:1000, Abcam), peroxiredoxin 1 (PRX1: LF-PA0001, 1:2000, Lab Frontier), PRX2 (LF-PA0007, 1:2000, Lab Frontier), PRX3 (LF-PA0030, 1:2000, Lab Frontier), PRX6 (ab16824, 1:1000, Abcam), PRX-SO₃ (LF-PA0004, 1:2000, Lab Frontier), PRX6-SO₃ (LF-PA0005, 1:2000, Lab Frontier), superoxide dismutase (SOD-1) (sc-11407, 1:100, Santa Cruz), SOD-2 (06-984, 1:500, Upstate), protein disulphide-isomerase (MA3-019, 1:1000, Affinity BioReagents), Mouse Total OXPHOS Complexes Detection kit (MS601m, 1:250, MitoSciences) and mitofilin (10179-1-AP, 1:400, Proteintech).

2.8 Cell viability

Cells were cultured on 96-well plates. After 48 h, cells were incubated with different concentrations of diethyl maleate (DEM, D97703, Sigma) or 2-mercaptoethanol for 24 h or with 100 µM 1,3-bis(2-chloroethyl)-1-nitrosourea (carmustine) (BCNU, C0400, Sigma) for 1, 3, 6 and 24 h. CellTiter 96[®] AQueous One Solution (Cell Proliferation Assay, Promega) was added with dilution ratio of 1:6 in DMEM. After 3 h incubation, the OD at 490 nm was recorded using a photometer [29].

2.9 Glutathione measurement

Cells were cultured on six-well plates. After 48 h, cells were washed briefly with PBS twice. Cold 6.5% TCA was added to each well (1 mL/well) and incubated on ice for 10 min. TCA extracts were transferred into Eppendorf tubes. 7.5 μ L of acid sample extract or acid GSH standard was added to 275 μ L of 80 mM KH_2PO_4 (pH 8.0) containing 5 mM EDTA, followed by 15 μ L of 0.1% w/v *o*-phthalaldehyde in methanol. After 25 min, fluorescence was measured on a Fusion™ universal microplate analyser (Packard) by using excitation and emission wavelengths of 350 and 420 nm, respectively. Adherent cell protein was solubilized by adding 1 mL of 0.5 M NaOH for 1 h [30]. Protein concentrations were determined using Bradford method [22].

2.10 ATP measurement

ATP was determined by using a bioluminescence assay. TCA extract (10 μ L) or acid ATP standard was added to 140 μ L of a 1:1:1 mixture of 80 mM $\text{MgSO}_4 \cdot 7\text{H}_2\text{O}$ /10 mM KH_2PO_4 /100 mM Na_2AsO_4 (pH 7.4) and mixed 50 μ L of firefly lantern extract solution (1 mg/mL, F3641, Sigma). Bioluminescence was measured by using a luminescence plate reader (Fusion universal microplate analyser, Packard) [30].

2.11 Glutathione reductase measurement

Cells were washed with PBS and lysed in a buffer containing 50 mM Tris and 5 mM EDTA (pH 7.5). Cell lysates were sonicated for 30 s and centrifuged at 13.2 krpm for 20 min at 4°C. The supernatants were analysed for glutathione (GSH) reductase activities by using a GSH reductase kit (Randox Laboratories) on Cobas Mira chemistry analyser (Roche). Enzymatic activities were adjusted for protein concentrations.

2.12 Mitochondrial superoxide and total reactive oxygen species (ROS) measurement

Cells were cultured in 24-well plates for 48 h, pretreated with 20 μ g/mL of antimycin A or 10 μ M rotenone for 3 h and incubated with 2.5 μ M MitoSOX™ Red mitochondrial superoxide indicator (M36008, Molecular Probes) and 10 μ M dihydrorhodamine 123 (DHR123, D632, Molecular Probes) in HBSS (14025-092, Invitrogen) for 30 min. After washing with HBSS, the plates were scanned on a fluorescence scanner (Typhoon 9400, GE healthcare) for excitation and emission wavelengths of 532 and 580 nm for MitoSOX and 488 and 520 nm for DHR123, respectively. Fluorescence intensity was quantified using the ImageQuant software (Molecular Dynamics).

2.13 Statistical analysis

Statistical analysis was performed using the analysis of variance and Student's *t*-test. Results were given as means \pm SEM. A *p*-value of less than 0.05 was considered significant.

3 Results

3.1 ES-derived SMCs

Murine ES cells were cultured in collagen-IV coated flasks and predifferentiated to Sca-1⁺ cells by the withdrawal of LIF. Subsequently, Sca-1⁺ cells were isolated by MACS. Stimulation by PDGF-BB (10 ng/mL) for five passages resulted in mRNA expression of smooth muscle α -actin, SM22, calponin and SMMHC (Fig. 1A). Verification by FACS analysis showed that more than 95% of esSMCs expressed SMC markers (Fig. 1B).

3.2 Proteomic analysis

To allow accurate quantification of protein expression in ES cell-derived SMCs and aortic SMCs, we used the DIGE approach: in brief, proteins were labelled with Cy3 or Cy5 and coseparated by 2-DE using a broad range pH gradient (pH 3–10 NL) and large format 12% SDS gels (Fig. 2). After normalization to the internal pooled standard labelled with Cy2, 146 spots showed a significant two-fold change ($p < 0.05$, $n = 6$ for esSMCs, $n = 2$ for aortic SMC) in the biological variation analysis module of the DeCyder software. One hundred and twenty-eight spots (88%) were successfully identified by MALDI-TOF MS or LC MS/MS (Supplementary Table 1).

While cytoskeletal/myofilament proteins and calcium-binding proteins were less abundant in esSMCs than in aortic SMCs, chaperones such as heat shock proteins were increased (Fig. 3A) along with proteins regulating DNA maintenance, transcription and translation. Notably, up-regulation of the cytosolic antioxidant PRX6 (spot 50) coincided with overoxidation of its redox-active cysteine (PRX6-SO₃) and a coordinated rise of other cytosolic members of the PRX family, *i.e.* PRX1 and PRX2, albeit less pronounced than PRX6. In contrast, the mitochondrial antioxidant PRX3 was down-regulated in esSMCs. Similarly, the reduction in mitochondrial manganese SOD (SOD-2, spots 77 and 78) was accompanied by an increase of the cytosolic copper-zinc SOD (SOD-1) in esSMCs as verified by immunoblotting (Fig. 3B). Notably, while certain differences, *i.e.* for chaperones such as heat shock protein 27 and crystalline α/β (Fig. 3C), were also present in undifferentiated ES cells, the differential expression of antioxidants appeared to be an intrinsic difference between the smooth muscle populations and was not detectable in undifferentiated ES cells (Fig. 3D).

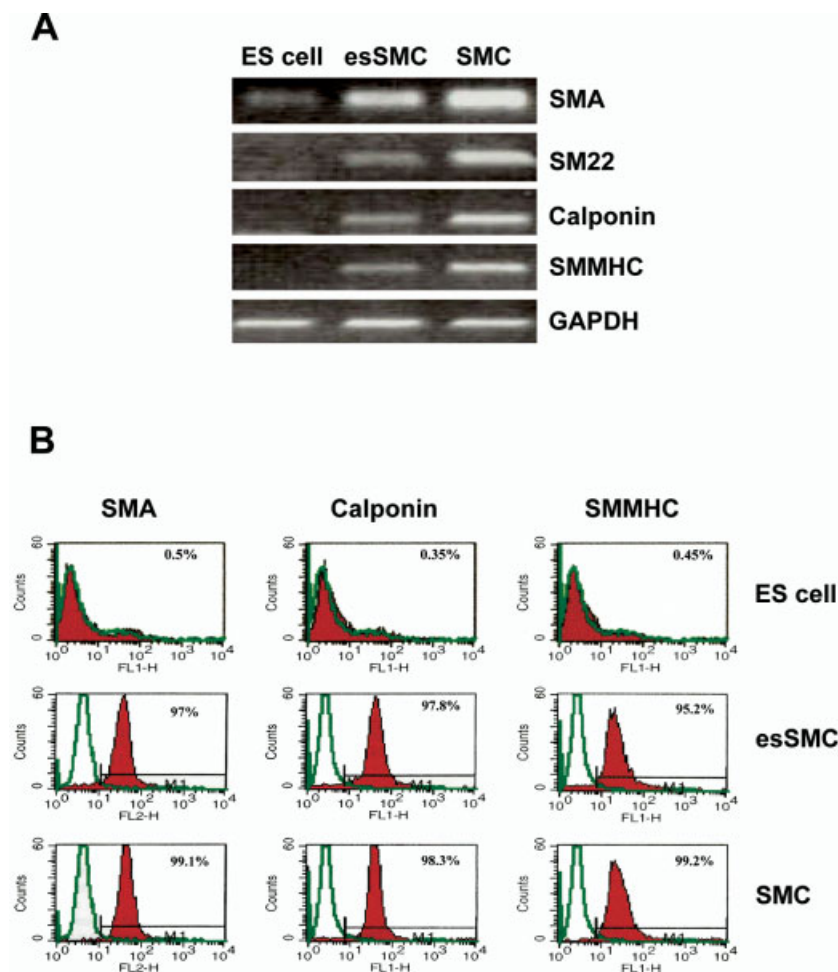


Figure 1. Verification of esSMCs. RT-PCR and FACS analysis of SMC specific markers in ES cells, esSMC and aortic SMCs. mRNA levels of SMC specific markers were detected by RT-PCR (A). GAPDH was used as a loading control. For FACS analysis, cells were incubated with either isotype controls (green line) or antibodies to SM-actin, calponin and SMMHC (red line) (B).

3.3 ROS production

The predominant cytosolic rather than mitochondrial antioxidant expression in esSMCs prompted us to study possible alterations in the subcellular redox state. We quantified total ROS and mitochondrial superoxide production by DHR123 and MitoSOX staining, respectively. The fluorescence signal intensity for DHR123 was higher in esSMCs compared to aortic SMCs as verified in cellular lysates using a fluorimeter (2133 ± 50 relative fluorescence unit (RFU)/ μg protein *vs.* 1782 ± 64 RFU/ μg protein, $p = 0.002$). Notably, the increase in total ROS production was accounted for by a rise in mitochondrial superoxide production as indicated by a corresponding increase in MitoSOX staining. To further clarify the site of ROS generation, we treated SMCs with rotenone and antimycin A, the inhibitors of mitochondrial complexes I and III, respectively. Antimycin A and not rotenone augmented mitochondrial superoxide (Fig. 4A) and total ROS (Fig. 4B) formation in esSMCs, but did not substantially alter the fluorescence signal of aortic SMCs. Further, Western blot analysis confirmed that complex III was more abundant in

esSMCs, while expression of complex I was decreased (Fig. 4C) providing additional proof that the observed increase in oxidative stress in esSMC is predominantly from mitochondria and that complex III might act as the principal site of ROS generation.

3.4 Cell viability

Notably, the rise in mitochondrial ROS in esSMCs was paired with a down-regulation of mitofilin, a mitochondrial inner membrane protein which regulates metabolic flux, decreased expression of ATP synthase beta chain (Supplementary Table 1) and a drop in cellular ATP levels (19.52 ± 1.07 $\mu\text{mol/g}$ proteins in esSMCs *vs.* 32.31 ± 1.10 $\mu\text{mol/g}$ proteins in aortic SMCs) (Fig. 5A). Moreover, esSMCs showed reduced concentrations of GSH, the major intracellular antioxidant (40.65 ± 0.52 $\mu\text{mol/g}$ protein in esSMCs *vs.* 49.87 ± 1.34 $\mu\text{mol/g}$ protein in aortic SMCs) (Fig. 5B), despite a compensatory increase of GSH reductase activity (107.6 ± 2.8 IU/g protein in esSMCs *vs.* 33.5 ± 1.1 IU/g protein in aortic SMCs) (Fig. 5C). esSMCs

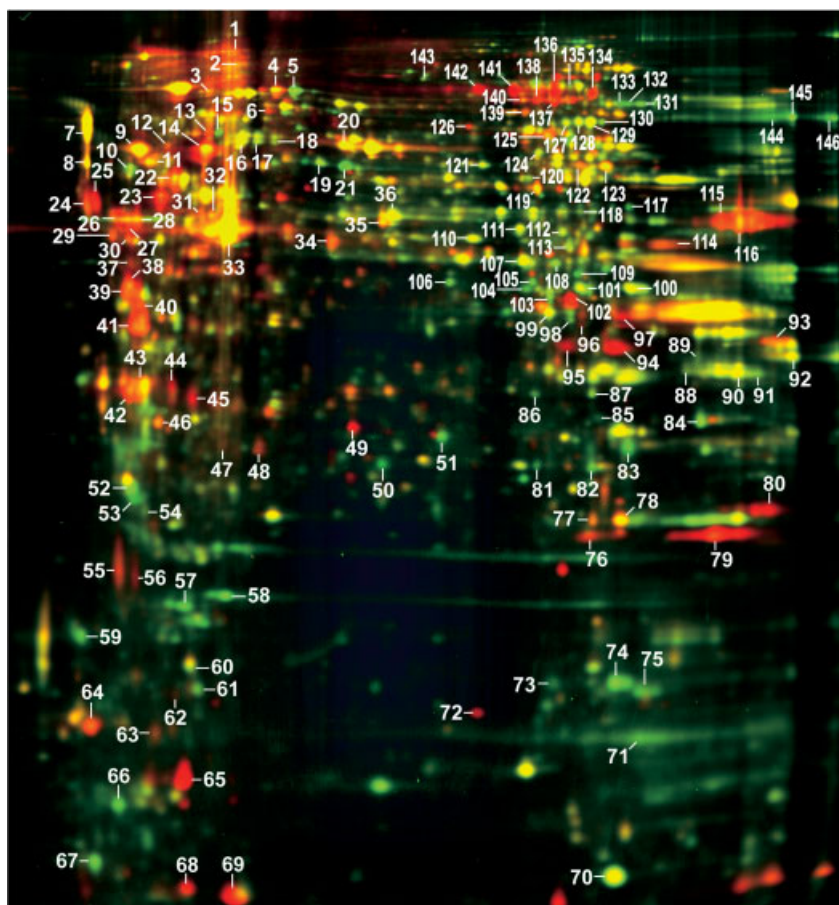


Figure 2. Proteomic analysis of esSMCs and aortic SMCs. esSMCs (green) and aortic SMCs (red) were compared using the DIGE approach. Protein lysates were labelled with Cy3 and Cy5, respectively, and coseparated in large format 2-DE gels. Images were acquired on a fluorescence scanner and analysed by DeCyder software. Spots with two-fold increase or decrease in esSMCs were numbered, picked and identified by MS.

were more susceptible to cell death upon treatment with DEM, a sulphhydryl-reactive agent that results in rapid depletion of GSH followed by a drop in ATP [31] and incubation with carmustine (BCNU), a GSH reductase inhibitor (Fig. 6A and B). In contrast, esSMCs' viability improved on addition of 2-mercaptoethanol to the culture medium (Fig. 6C) highlighting their need for additional antioxidant protection.

4 Discussion

Stem cell research holds great promise for regenerative medicine and tissue engineering and provides exciting new avenues for treating cardiovascular diseases. A number of studies demonstrated that vascular progenitor cells, including endothelial and smooth muscle progenitors are present in circulating blood and have the capacity to differentiate into mature SMCs and endothelial cells [4, 6, 32–35], thereby contributing to vascular repair, remodelling and atherosclerotic lesion formation [5, 36–38]. It is also established that ES cells can differentiate into SMCs *in vitro* [3], but associated protein changes remain to be elucidated. In the present study, we present the first proteomic comparison of

murine aortic SMCs and esSMCs demonstrating that the latter encounter increased oxidative stress due to a rise in mitochondrial-derived ROS, making them more susceptible to oxidative stress-induced cell death despite a compensatory increase in their endogenous antioxidant defence capacities. Thus, differences in protein expression relate to their altered cell function, and maintaining the balance between ROS generation and antioxidative scavenging will be essential for the longevity of esSMCs and their potential use in tissue engineering.

4.1 Oxidative stress in stem cells

It has recently been shown that adult endothelial progenitor cells (EPCs) have increased antioxidant protection [39], that oxidative stress accelerates endothelial progenitor cell senescence [40] and that mice deficient for GSH peroxidase have dysfunctional EPCs with impaired ability to promote angiogenesis [41]. Our data presented in this study show higher levels of antioxidants in esSMCs, indicating that esSMCs share some similarities with adult progenitor cells. However, oxidative stress is determined by the balance between pro-oxidants and antioxidants, and alterations in individual ROS

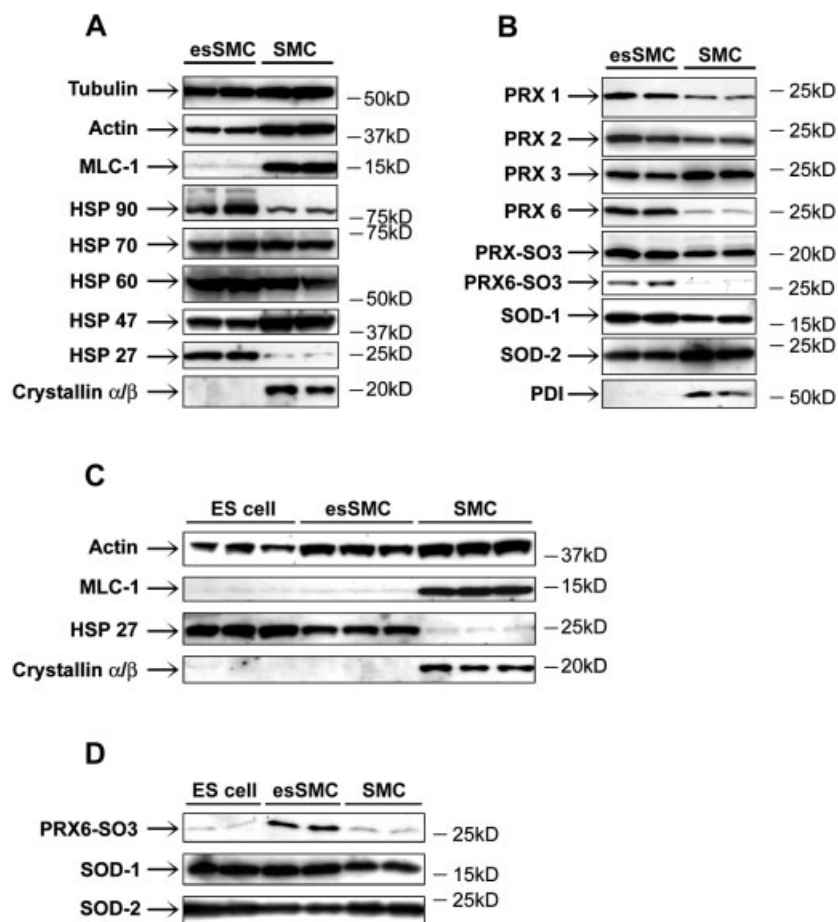


Figure 3. Immunoblotting. Differences in protein expression for chaperones and structural proteins were analysed by immunoblotting (A). Expression levels of antioxidants in esSMCs and aortic SMCs (B). Note that cytosolic antioxidants (PRX1, 2, 6, SOD-1) were increased, while mitochondrial antioxidants (PRX3, SOD-2) were decreased in esSMCs and the redox-active cysteines of PRXs were predominantly oxidized ($-\text{SO}_3$), indicating increased oxidative stress. While some differences, *e.g.* for chaperones (C), were also present in undifferentiated ES cells, the changes in antioxidants were an intrinsic characteristic of esSMCs (D). MLC, myosin light chain; PRX, peroxiredoxin; PRX-SO₃, oxidized form of PRX1–4; PRX6-SO₃, oxidized form of PRX6; SOD, superoxide dismutase; PDI, protein disulphide-isomerase.

generating enzymes are likely to be compensated for by synergistic ones. To understand such complex biological systems, a more comprehensive approach is needed and proteomics offers the possibility to simultaneously assess the expression of multiple pro- and antioxidants [42].

4.2 Source of ROS and expression of antioxidants

In human blood vessels, the membrane-associated NAD(P)H oxidase is thought to be the principal source of superoxide and functionally related to cardiovascular risk factors [43, 44]. Besides its predominant role in the respiratory burst oxidation of inflammatory cells, NADPH oxidase is also responsible for excess ROS production in vascular SMCs [45]. But unlike mature SMCs, mitochondria appear to be the major source of excess ROS in esSMCs. Notably, the normal function of complex III of the electron transport chain was previously found to be essential for ES cell differentiation to cardiomyocytes [46]. We now demonstrate that complex III is more abundant in esSMCs, contributing to a marked increase in mitochondria-derived free radicals. These alterations in the mitochondrial redox state were

accompanied by a reduction in mitochondrial antioxidants, and a compensatory up-regulation of cytosolic ROS scavenging enzymes in esSMCs. But the coordinated rise in cytosolic antioxidative defence capacity was unable to compensate for the loss of mitochondrial antioxidants, and to provide sufficient protection. esSMCs remained more susceptible to oxidative injury and depletion of intracellular GSH or inhibition of GSH reductase resulted in a pronounced loss of cell viability.

4.3 Energy metabolism

It is noteworthy that the alterations in mitochondrial redox status were associated with a reduction in ATP synthase expression and a drop in cellular ATP level. This is in agreement with our previous observations in aortas of Apolipoprotein E deficient mice, where a depletion of vascular energy metabolites coincided with increased oxidative stress while attenuated lesion formation was associated with reduced oxidative stress and successful recovery of the energy pool [47]. We now demonstrate that increased oxidative stress in esSMCs is associated with abnormal mito-

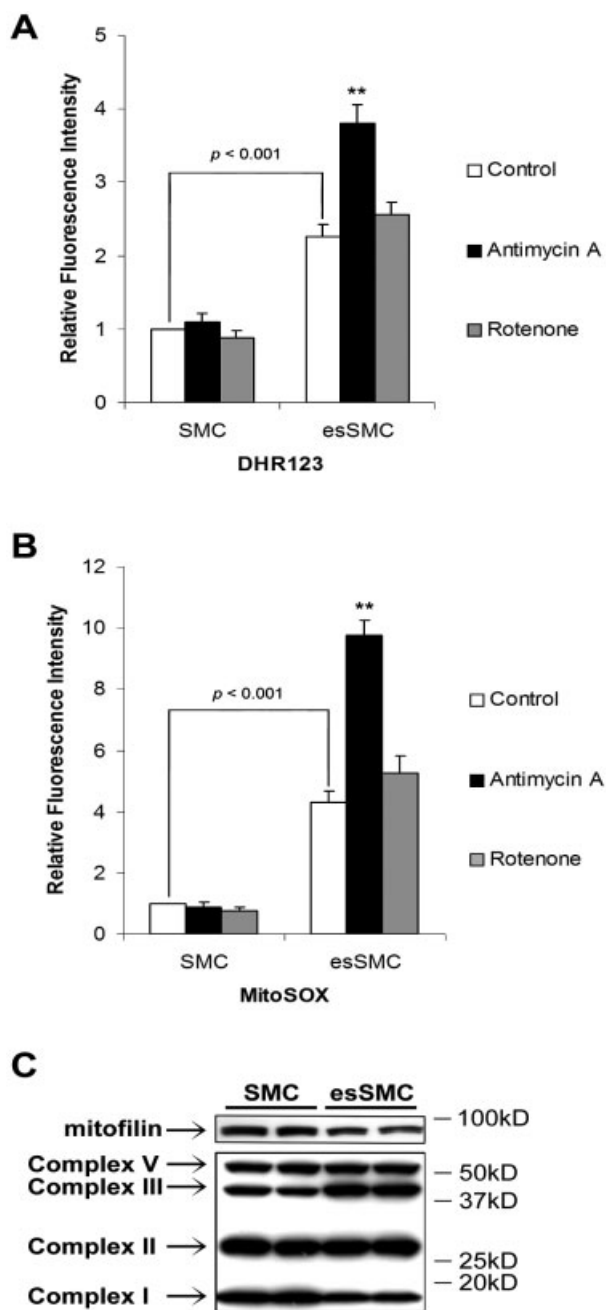


Figure 4. Measurement of ROS. DHR123 (A) and MitoSOX staining (B) were used to assess total ROS and mitochondrial superoxide production in esSMCs and aortic SMCs. Note that esSMCs show a significant rise in mitochondrial superoxide production. Changes in oxidative stress were analysed after treatment with rotenone and antimycin A, the inhibitors of complexes I and III, respectively. Note that the complex III inhibitor antimycin A resulted in a marked increase in mitochondrial superoxide production in esSMCs. ** $p < 0.01$ compared to control. Western blots demonstrate an increase of electron transport chain complex III and less complex I and mitofilin expression in esSMCs (C). Representative subunits for mitochondrial OXPHOS complexes: complex I (20 kDa subunit), complex II (30 kDa lp subunit), complex III (core 2) and complex V (ATP synthase $F_1\alpha$).

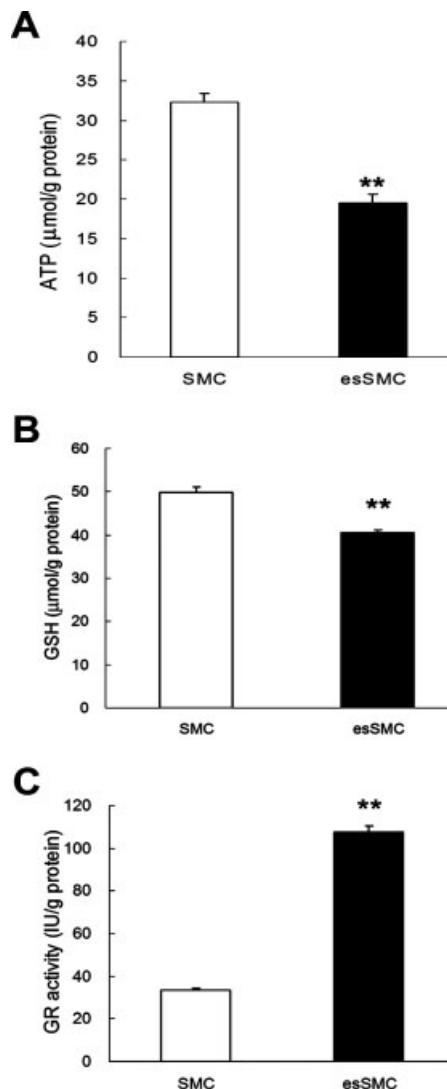


Figure 5. Cellular ATP, GSH and GSH reductase. Comparison of cellular ATP levels (A), concentrations of reduced GSH (B) and GSH reductase activity (C) in esSMCs and aortic SMCs.

chondrial function as evidenced by expression changes in respiratory chain complexes and a drop in cellular ATP [48]. Similarly, others have shown that overexpression of the uncoupling protein 1 promotes atherosclerosis by triggering mitochondrial dysfunction, depleting energy stores and increasing superoxide production [49]. Thus, there is a growing body of evidence that mitochondrial energy metabolism and oxidative stress are intertwined in cardiovascular disease.

4.4 Limitations of the study

The lack of specific cell markers is one of the most pressing problems in stem cell research [50, 51]. In the present study, we used a panel of marker proteins, which are commonly

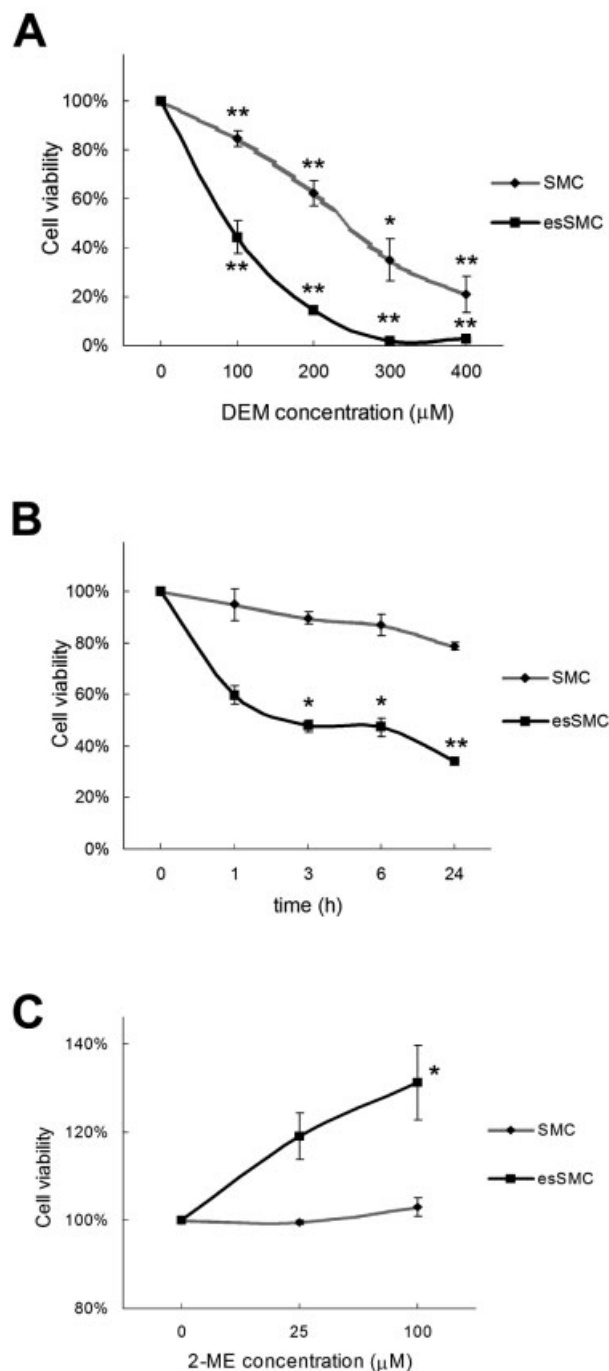


Figure 6. Cell viability. Cell viability after depletion of GSH by treatment with DEM (A) or inhibition of GSH reductase by carmustine (BCNU) (B). Increase in esSMC survival upon addition of 2-mercaptoethanol to the culture medium (C). * $p < 0.05$ compared to baseline, ** $p < 0.01$.

used to verify vascular SMCs in culture. As all these proteins also exist in non-vascular SMCs, we cannot rule out the presence of SMCs from other origins among the esSMC population. The RT-PCR primers for the detection of SMA

and SM22, however, were vascular specific. Importantly, although esSMCs express the same marker proteins currently used to define mature vascular SMCs [52] and vascular SMC progenitors among mononuclear cell populations [6], their proteome and function were very different. Thus, the expression of SMC markers may be indicative but not sufficient to characterize stem cell-derived cells, and proteomics may offer an opportunity to progress towards a molecular classification of stem cell-derived cells based on comparative analysis of protein expression patterns, rather than relying on the expression of a selected panel of marker proteins.

5 Conclusion

We present the first proteomic comparison of murine aortic SMCs and esSMCs, demonstrating that there is a requirement to define stem cell populations by proteomics for a systematic understanding of changes occurring during development. We expect that our identification of differentially expressed proteins during stem cell differentiation may have implications in stem cell therapy and tissue engineering.

The use of the facilities of the Medical Biomics Centre (St. George's, University of London) is gratefully acknowledged. We thank Dr. Salim Fredericks (Analytical Unit, Department of Cardiac and Vascular Sciences, St. George's, University of London) for technical assistance. This work was supported by grants from the British Heart Foundation and Oak Foundation.

6 References

- [1] Evans, M. J., Kaufman, M. H., *Nature* 1981, 292, 154–156.
- [2] Martin, G. R., *Proc. Natl. Acad. Sci. USA* 1981, 78, 7634–7638.
- [3] Drab, M., Haller, H., Bychkov, R., Erdmann, B. *et al.*, *FASEB J.* 1997, 11, 905–915.
- [4] Shimizu, K., Sugiyama, S., Aikawa, M., Fukumoto, Y. *et al.*, *Nat. Med.* 2001, 7, 738–741.
- [5] Saiura, A., Sata, M., Hirata, Y., Nagai, R., Makuuchi, M., *Nat. Med.* 2001, 7, 382–383.
- [6] Simper, D., Stalboerger, P. G., Panetta, C. J., Wang, S., Caplice, N. M., *Circulation* 2002, 106, 1199–1204.
- [7] Hu, Y., Zhang, Z., Torsney, E., Afzal, A. R. *et al.*, *J. Clin. Invest.* 2004, 113, 1258–1265.
- [8] Kim, B. S., Nikolovski, J., Bonadio, J., Mooney, D. J., *Nat. Biotechnol.* 1999, 17, 979–983.
- [9] Kim, B. S., Nikolovski, J., Bonadio, J., Smiley, E., Mooney, D. J., *Exp. Cell Res.* 1999, 251, 318–328.
- [10] Cho, S. W., Kim, I. K., Lim, S. H., Kim, D. I. *et al.*, *Biomaterials* 2004, 25, 2979–2986.
- [11] McKee, J. A., Banik, S. S., Boyer, M. J., Hamad, N. M. *et al.*, *EMBO Rep.* 2003, 4, 633–638.

- [12] Nikolovski, J., Kim, B. S., Mooney, D. J., *FASEB J.* 2003, *17*, 455–457.
- [13] Grassl, E. D., Oegema, T. R., Tranquillo, R. T., *J. Biomed. Mater. Res.* 2002, *60*, 607–612.
- [14] Mayr, M., Mayr, U., Chung, Y. L., Yin, X. *et al.*, *Proteomics* 2004, *4*, 3751–3761.
- [15] McGregor, E., Kempster, L., Wait, R., Welson, S. Y. *et al.*, *Proteomics* 2001, *1*, 1405–1414.
- [16] Dupont, A., Corseaux, D., Dekeyser, O., Drobecq, H. *et al.*, *Proteomics* 2005, *5*, 585–596.
- [17] Mayr, U., Mayr, M., Yin, X., Begum, S. *et al.*, *Proteomics* 2005, *5*, 4546–4557.
- [18] Yin, X., Mayr, M., Xiao, Q., Mayr, U. *et al.*, *Proteomics* 2005, *5*, 4533–4545.
- [19] Unlu, M., Morgan, M. E., Minden, J. S., *Electrophoresis* 1997, *18*, 2071–2077.
- [20] Vittet, D., Prandini, M. H., Berthier, R., Schweitzer, A. *et al.*, *Blood* 1996, *88*, 3424–3431.
- [21] Hu, Y., Zou, Y., Dietrich, H., Wick, G., Xu, Q., *Circulation* 1999, *100*, 861–868.
- [22] Bradford, M. M., *Anal. Biochem.* 1976, *72*, 248–254.
- [23] Yan, J. X., Wait, R., Berkelman, T., Harry, R. A. *et al.*, *Electrophoresis* 2000, *21*, 3666–3672.
- [24] Shevchenko, A., Wilm, M., Vorm, O., Mann, M. *Anal. Chem.* 1996, *68*, 850–858.
- [25] Perkins, D. N., Pappin, D. J., Creasy, D. M., Cottrell, J. S., *Electrophoresis* 1999, *20*, 3551–3567.
- [26] Wilm, M., Shevchenko, A., Houthaeve, T., Breit, S. *et al.*, *Nature* 1996, *379*, 466–469.
- [27] Li, C., Hu, Y., Mayr, M., Xu, Q., *J. Biol. Chem.* 1999, *274*, 25273–25280.
- [28] Li, C., Hu, Y., Sturm, G., Wick, G., Xu, Q., *Arterioscler. Thromb. Vasc. Biol.* 2000, *20*, E1–E9.
- [29] Mayr, U., Mayr, M., Li, C., Wernig, F. *et al.*, *Circ. Res.* 2002, *90*, 197–204.
- [30] Jenner, A. M., Ruiz, J. E., Dunster, C., Halliwell, B. *et al.*, *Arterioscler. Thromb. Vasc. Biol.* 2002, *22*, 574–580.
- [31] Mayr, M., Siow, R., Chung, Y. L., Mayr, U. *et al.*, *Circ. Res.* 2004, *94*, e87–e96.
- [32] Asahara, T., Murohara, T., Sullivan, A., Silver, M. *et al.*, *Science* 1997, *275*, 964–967.
- [33] Rafii, S., *J. Clin. Invest.* 2000, *105*, 17–19.
- [34] Hu, Y., Davison, F., Ludewig, B., Erdel, M. *et al.*, *Circulation* 2002, *106*, 1834–1839.
- [35] Hu, Y., Mayr, M., Metzler, B., Erdel, M. *et al.*, *Circ. Res.* 2002, *91*, e13–e20.
- [36] Han, C. I., Campbell, G. R., Campbell, J. H., *J. Vasc. Res.* 2001, *38*, 113–119.
- [37] Hillebrands, J. L., Klatter, F. A., van den Hurk, B. M., Popa, E. R. *et al.*, *J. Clin. Invest.* 2001, *107*, 1411–1422.
- [38] Sata, M., *Trends Cardiovasc. Med.* 2003, *13*, 249–253.
- [39] Dernbach, E., Urbich, C., Brandes, R. P., Hofmann, W. K. *et al.*, *Blood* 2004, *104*, 3591–3597.
- [40] Imanishi, T., Hano, T., Nishio, I., *J. Hypertens* 2005, *23*, 97–104.
- [41] Galasso, G., Schiekofer, S., Sato, K., Shibata, R. *et al.*, *Circ. Res.* 2006, *98*, 254–261.
- [42] Mayr, M., Zhang, J., Greene, A. S., Gutterman, D. D. *et al.*, *Mol. Cell. Proteomics* 2006, *5*, 1853–1864.
- [43] Griendling, K. K., FitzGerald, G. A., *Circulation* 2003, *108*, 1912–1916.
- [44] Griendling, K. K., FitzGerald, G. A., *Circulation* 2003, *108*, 2034–2040.
- [45] West, N., Guzik, T., Black, E., Channon, K., *Arterioscler. Thromb. Vasc. Biol.* 2001, *21*, 189–194.
- [46] Spitkovsky, D., Sasse, P., Kolossov, E., Bottinger, C. *et al.*, *FASEB J.* 2004, *18*, 1300–1302.
- [47] Mayr, M., Chung, Y. L., Mayr, U., Yin, X. *et al.*, *Arterioscler. Thromb. Vasc. Biol.* 2005, *25*, 2135–2142.
- [48] John, G. B., Shang, Y., Li, L., Renken, C. *et al.*, *Mol. Biol. Cell* 2005, *16*, 1543–1554.
- [49] Bernal-Mizrachi, C., Gates, A. C., Weng, S., Imamura, T. *et al.*, *Nature* 2005, *435*, 502–506.
- [50] Hristov, M., Weber, C., *J. Cell. Mol. Med.* 2004, *8*, 498–508.
- [51] Xu, Q., *Nat. Clin. Pract. Cardiovasc. Med.* 2006, *3*, 94–101.
- [52] Owens, G. K., Kumar, M. S., Wamhoff, B. R., *Physiol. Rev.* 2004, *84*, 767–801.